

DAFTAR PUSTAKA

- Almadhoni, K., & Khan, S. (2015). Evaluation of the Effective Thermal Properties of Aluminum Metal Matrix Composites Reinforced by Ceramic Particles. *International Journal of Current Engineering and Technology*, 5(4), 15.
- Alvarez, A., Cabeza, O., Muniz, M. C., & Varela, L. M. (2010). Experimental and numerical investigation of a flat-plate solar collector. *Energy*, 35, 3707–3716.
- Bhowmik, H., & Amin, R. (2017). Efficiency improvement of flat plate solar collector using reflector. *Energy Reports*, 3, 119–123.
- Bouhal, T., El Rhafiki, T., Kousksou, T., Jamil, A., & Zeraouli, Y. (2018). PCM addition inside solar water heaters: Numerical comparative approach. *Journal of Energy Storage*, 19, 232–246. <https://doi.org/10.1016/j.est.2018.08.005>
- Chen, C. C., & Huang, P. C. (2012). Numerical study of heat transfer enhancement for a novel flat-plate solar water collector using metal-foam blocks. *International Journal of Heat and Mass Transfer*, 55(23–24), 6734–6756.
- Chong, K. K., Chay, K. G., & Chin, K. H. (2012). Study of a solar water heater using stationary V-trough collector. *Renewable Energy*, 39, 207–215.
- Dovic, D., & Andrassy, M. (2012). Numerically assisted analysis of flat and corrugated plate solar collectors thermal performances. *Solar Energy*, 86, 2416–2431.
- El-Kady, E.-S. Y., Mahmoud, T. S., & Ali, A. (2011). On the Electrical and Thermal Conductivities of Cast A356/Al₂O₃ Metal Matrix Nanocomposites. *Materials Sciences and Applications*, 2, 1180–1187.
- Eltaweel, M., & Abdel-Rehim, A. A. (2019). Energy and exergy analysis of a thermosiphon and forced-circulation flat-plate solar collector using MWCNT/Water nanofluid. *Case Studies in Thermal Engineering*, 14, 100416. <https://doi.org/10.1016/j.csite.2019.100416>
- Fan, M., You, S., Gao, X., Zhang, H., Li, B., Zheng, W., Sun, L., & Zhou, T. (2019). A comparative study on the performance of liquid flat-plate solar

collector T with a new V-corrugated absorber. *Energy Conversion and Management*, 184, 235–248.

- Faraj, K., Khaled, M., Faraj, J., Hachem, F., & Castelain, C. (2021). A review on phase change materials for thermal energy storage in buildings: Heating and hybrid applications. *Journal of Energy Storage*, 33, 101913. <https://doi.org/10.1016/j.est.2020.101913>
- Furukawa, M., Wang, J., Horita, Z., & Nemoto, M. (1995). The Mechanical Properties of an Aluminum Composite Reinforced with Alumina Microsphere. *Key Engineering Materials*, 104–107, 817–824.
- Haddada, J., Arif, E., Halim, A., & Tarakka, R. (2017). The Performance of Solar Water Heater System using Integrated Collector and PCM Energy Storage. *Prosiding SNTTM XVI*, 5.
- He, W. (2018). Design of a two-medium solar collector in residential buildings. *Energy Procedia*, 152, 456–461. <https://doi.org/10.1016/j.egypro.2018.09.253>
- Jalaluddin, Effendy, A., & Tarakka, R. (2016). Experimental Study of an SWH System with V-Shaped Plate. *J. Eng. Technol. Sci*, 48(2), 207–217.
- Jalaluddin, & Miyara, A. (2016). Thermal Performances Of Vertical Ground Heat Exchangers In Different Conditions. *Journal of Engineering Science and Technology*, 11(12), 13.
- Jalaluddin, Miyara, A., Ishikawa, S., Tarakka, R., & Amijoyo Mochtar, A. (2018). Development of an open-loop ground source cooling system for space air conditioning system in hot climate like Indonesia. *MATEC Web of Conferences*, 204, 04007. <https://doi.org/10.1051/mateconf/201820404007>
- Jalaluddin, Tarakka, R., & Miyara, A. (2018). Performance of Shallow Borehole of spiral-Tube Ground Heat Exchanger. *Journal of Mechanical Engineering*, 15(2), 12.
- Kalogirou, S. A. (2004). *Solar thermal collectors and applications*. 30, 231–295. <https://doi.org/10.1016/j.peccs.2004.02.001>
- O’Hegarty, R., Kinnane, O., & McCormack, S. J. (2017). Concrete solar collectors for façade integration: An experimental and numerical investigation. *Applied Energy*, 206, 1040–1061. <https://doi.org/10.1016/j.apenergy.2017.08.239>

- Oliveira, F. A. C., Fernandes, J. C., Galindo, J., Rodríguez, J., Canãdas, I., & Rosa, I. G. (2019). Thermal resistance of solar volumetric absorbers made of mullite, brown alumina and ceria foams under concentrated solar radiation. *Solar Energy Materials and Solar Cells*, *194*, 121–129.
- Popel, O. S., Frid, S. E., Mordynskii, A. V., Suleimanov, M. Zh., Arsatov, A. V., & Oschepkov, M. Yu. (2013). Results of the development of a solar accumulation-type water heater made of polymer and composite materials. *Thermal Engineering*, *60*(4), 267–269. <https://doi.org/10.1134/S0040601513040101>
- Rangababu, J. A., Kumar, K., & Rao, S. (2015). Numerical Analysis and Validation of Heat Transfer Mechanism of Flat Plate Collectors. *Procedia Engineering*, *127*, 63–70.
- Saad, H. E., Kaddah, K. S., Sliem, A. A., Rafat, A., & Hewhy, M. A. (2019). The effect of the environmental parameters on the performance of asphalt solar collector. *Ain Shams Engineering Journal*, *10*(4), 791–800. <https://doi.org/10.1016/j.asej.2019.04.005>
- Saedodin, S., Zamzamian, S. A. H., Nimvari, M. E., Wongwises, S., & Jouybari, H. J. (2017). Performance evaluation of a flat-plate solar collector filled with porous metal foam_ Experimental and numerical analysis. *Energy Conversion and Management*, *153*, 278–287.
- Sakhrieh, A., & Al-Ghandoor, A. (2013). Experimental investigation of the performance of five types of solar collectors. *Energy Conversion and Management*, *65*, 715–720. <https://doi.org/10.1016/j.enconman.2011.12.038>
- Saravanan, A., Senthilkumar, J. S., & Jaisankar, S. (2016). Performance assessment in V-trough solar water heater fitted with square and V-cut twisted tape inserts. *Applied Thermal Engineering*, *38*.
- Shukla, R., Sumathy, K., Erickson, P., & Gong, J. (2013). Recent advances in the solar water heating systems: A review. *Renewable and Sustainable Energy Reviews*, *19*, 173–190. <https://doi.org/10.1016/j.rser.2012.10.048>
- Singh, P., Sharma, R. K., Ansu, A. K., & Goyal, R. (2020). Study on thermal properties of organic phase change materials for energy storage. *Materials Today: Proceedings*, *28*, 2353–2357. <https://doi.org/10.1016/j.matpr.2020.04.640>
- Stadler, C., & Lasova, V. (2005). Metal Foams – A New Promising Material For Engineering Design Applications. *AEDS*, *9*.

- Sun, X.-Y., Sun, X.-D., Li, X.-G., Wang, Z.-Q., He, J., & Wang, B.-S. (2014). Performance and building integration of all-ceramic solar collectors. *Energy and Buildings*, *75*, 176–180. <https://doi.org/10.1016/j.enbuild.2014.01.045>
- Tewari, K., & Dev, R. (2019). Exergy, environmental and economic analysis of modified domestic solar water heater with glass-to-glass PV module. *Energy*. <https://doi.org/10.1016/j.energy.2018.12.122>
- Valizade, M., Heyhat, M. M., & Maerefat, M. (2020). Experimental study of the thermal behavior of direct absorption parabolic trough collector by applying copper metal foam as volumetric solar absorption. *Renewable Energy*, *145*, 261–269.
- Yang, Y., Cao, S., Xu, J., & Cai, B. (2013). All-ceramic solar collectors. *Ceramics International*, *39*(5), 6009–6012. <https://doi.org/10.1016/j.ceramint.2013.01.011>
- Zukowski, M., & Woroniak, G. (2017). Experimental testing of ceramic solar collectors. *Solar Energy*, *146*, 532–542. <https://doi.org/10.1016/j.solener.2017.03.022>

Lampiran

Lampiran 1. Biodata Penulis

BIODATA

A. Data Pribadi

1. Nama : Muhammad Hasan Basri
2. Tempat, tanggal lahir : Tosora, 6 September 1977
3. Alamat : Jl. Soekarno-Hatta, Palu, Sulawesi Tengah
4. Kewarganegaraan : Warga Negara Indonesia

B. Riwayat Pendidikan

1. Tamat SMU Tahun 1995 di SMAN 5 Makassar
2. Sarjana (S1) Tahun 2000 di Universitas Hasanuddin
3. Magister (S2) Tahun 2007 di Universitas Hasanuddin

C. Pekerjaan dan Riwayat Pekerjaan

1. Pekerjaan : ASN di Universitas Tadulako
2. NIP : 197709062005011002
3. Pangkat / Jabatan : Penata Tk. I / III.d / Lektor

D. Karya ilmiah yang telah dipublikasikan

1. Basri, M. H., Jalaluddin, Tarakka, R., Syahid, M., & Ramadhan, M. A. I. (2022). Experimental Study of Modified Absorber Plate Integrated with Aluminium Foam of Solar Water Heating System. *International Journal of Renewable Energy Research*, 12(2), 993–999. <https://doi.org/10.20508/ijrer.v12i2.12930.g8482>
2. Basri, M. H., Jalaluddin, Tarakka, R., Syahid, M., & Ramadhan, M. A. I. (2023). Study of Modified Absorber Plate with Aluminium Foam of Solar Water Heating System. *Applied Mechanics and Materials*. Vol. 913, pp 45-51.

E. Makalah pada Seminar/Konferensi Ilmiah Nasional dan Internasional

1. Basri, M. H., Jalaluddin, Tarakka, R., Syahid, M., & Ramadhan, M. A. I. (2021). Study of Modified Absorber Plate with Aluminium Foam of Solar Water Heating System. Proceeding of the 5th International Conferences on Mechanical Engineering, 25-26 Agust 2021. Surabaya, Indonesia.
2. Jalaluddin, Tarakka, R., Syahid, M., Basri, M. H., & Ramadhan, M. A. I. (2021). Study of Solar Water Heater using Absorber Plate Integrated with Composite Thermal Storage. Proceeding of the International Conferences on the Energy, Manufacture, Advance material and Mechatronics, 23 Nov 2021. Makassar, Indonesia.
3. Basri, M. H., Jalaluddin, Tarakka, R., Syahid, M., & Ramadhan, M. A. I. Katjo, M.B. (2022). Thermal Properties Characteristic of Aluminium-Alumina Composite for Solar Water Heating System Application. Proceeding of the International Symposium on Advance and Innovation in Mechanical Engineering, 13 Okt 2022. Makassar, Indonesia.

Lampiran 2. Tabel Perhitungan Densitas Teoritis

Perhitungan Densitas Teoritis Komposit Aluminium-Alumina

Komposisi persentase penguat	Aluminium			Alumina			Komposit
	ρ_m	w_m	v_m	ρ_r	w_r	v_r	ρ
	gr/cm ³			gr/cm ³			gr/cm ³
35 %	2.75	0.65	0.7309	3.8	0.35	0.2690	3.036
50 %	2.75	0.5	0.5939	3.8	0.5	0.4060	3.208
65%	2.75	0.35	0.4406	3.8	0.65	0.5593	3.399

Persamaan densitas teoritis:

$$\rho_{\text{teoritis}} = \rho_m w_m + \rho_r w_r$$

Persamaan fraksi volume :

$$v_m = \left(\frac{\frac{w_m}{\rho_m}}{\frac{w_m}{\rho_m} + \frac{w_r}{\rho_r}} \right) \times 100\%$$

Lampiran 3. Data Temperature Konduktivitas Termal

PENGUJIAN KONDUKTIVITAS THERMAL

1 September 2022

Laboratorium Perpindahan Kalor dan Massa

Setiap pengujian bahan Dilakukan selama 30 menit

Pengujian bahan sebanyak 3 set.

Temperatur masing2 diseting 100° C.

DATA PENGUJIAN : 1, A1 (4 mm) (AL 35 A65)

A2 (2 mm) (AL 35 A 65)

Temperatur (°C)	Titik Pengambilan Data									
	T1	T2	T3	T4	T5	T6	T7	T8	T9	T10
	94.4	93.9	93.4	93.0	61.1	60.6	28.3	27.9	27.7	27.3

DATA PENGUJIAN : 2, B1 (4 mm) (AL 50 A50)

B2 (2 mm) (AL 50 A 50)

Temperatur (°C)	Titik Pengambilan Data									
	T1	T2	T3	T4	T5	T6	T7	T8	T9	T10
	94.3	93.8	93.2	92.6	59.6	59.0	28.8	28.3	27.9	27.6

DATA PENGUJIAN : 3, C1 (4 mm) (AL 65 A35)

C2 (2 mm) (AL 65 A 35)

Temperatur (°C)	Titik Pengambilan Data									
	T1	T2	T3	T4	T5	T6	T7	T8	T9	T10
	94.3	93.7	93.1	92.5	43.1	42.6	29.2	28.7	28.3	27.8

Lampiran 4. Data Hasil Pengujian Kapasitas Panas



**LABORATORIUM PENELITIAN DAN
PENGUJIAN TERPADU UNIVERSITAS
GADJAH MADA
LPPT UGM**

Jl. Kalurang KM. 4 Sekip Utara Yogyakarta 55281 Indonesia
Telp./Fax +62 274 548348 SMS. 082328276111 email : lppt_info@mail.ugm.ac.id

**LEMBAR KERJA UJI
ANALISIS TERMAL**

IDENTITAS SAMPEL

No. Sampel	22080101343	Tanggal Diterima	
Nama Sampel	Komposit	Tanggal Pengujian	
Kode Sampel	22080101343	Tanggal Selesai	01 September 22
Jumlah Sampel	3	Metode Uji	DSC

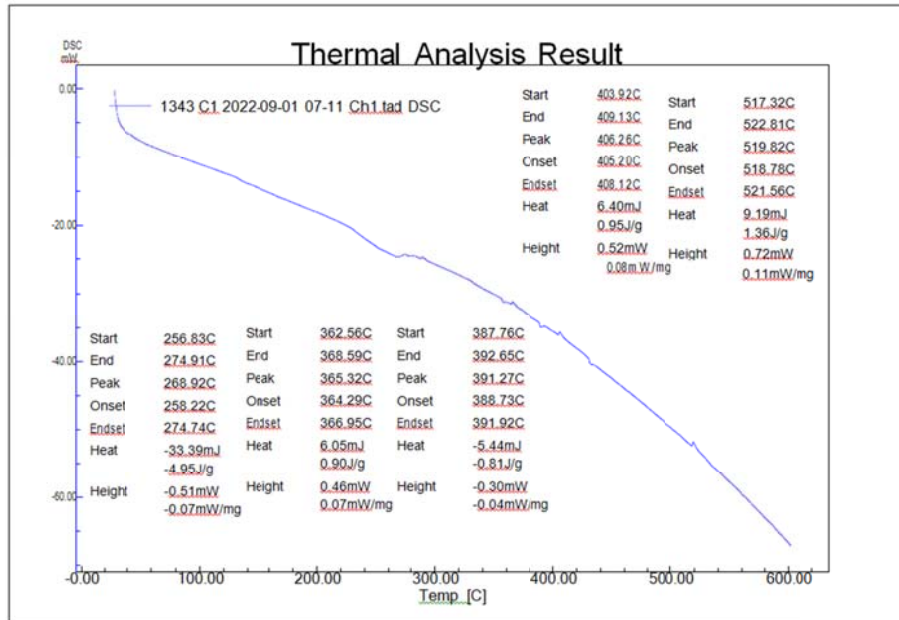
LAMPIRAN HASIL ANALISIS

1. C1

[File Information]		[Temp Program]	
File Name:	1343 C1 2022-09-01 07-11 Ch1.tad	Start Temp [°C]	30
Sample Name:	C1	Temp Rate [°C/min]	10
Lot No:	1343	Hold Temp [°C]	600
Acquisition Date	2022/09/01	Hold Time [min]	0
Acquisition Time	07:11:21(+0700)	Gas	Nitrogen
Detector:	DSC-60		
Serial No:	C30935200137SA		
Operator:	Heri		
Atmosphere:	Nitrogen		
Flow Rate:	10[ml/min]		
Cell:	Aluminum Crimping		
Sample Weight:	6.750[mg]		
Molecular Weight:	0.00		

[Analysis Result]

[DSC Peak]	1	2	3	4	5
Peak					
[°C]	268.92	365.32	391.27	406.26	519.82
Onset					
[°C]	258.22	364.29	388.73	405.20	518.78
Endset					
[°C]	274.74	366.95	391.92	408.12	521.56
Heat					
mJ	-33.39	6.05	-5.44	6.40	9.19
J/g	-4.95	0.90	-0.81	0.95	1.36
Height					
mW	-0.51	0.46	-0.30	0.52	0.72
mW/mg	-0.07	0.07	-0.04	0.08	0.11

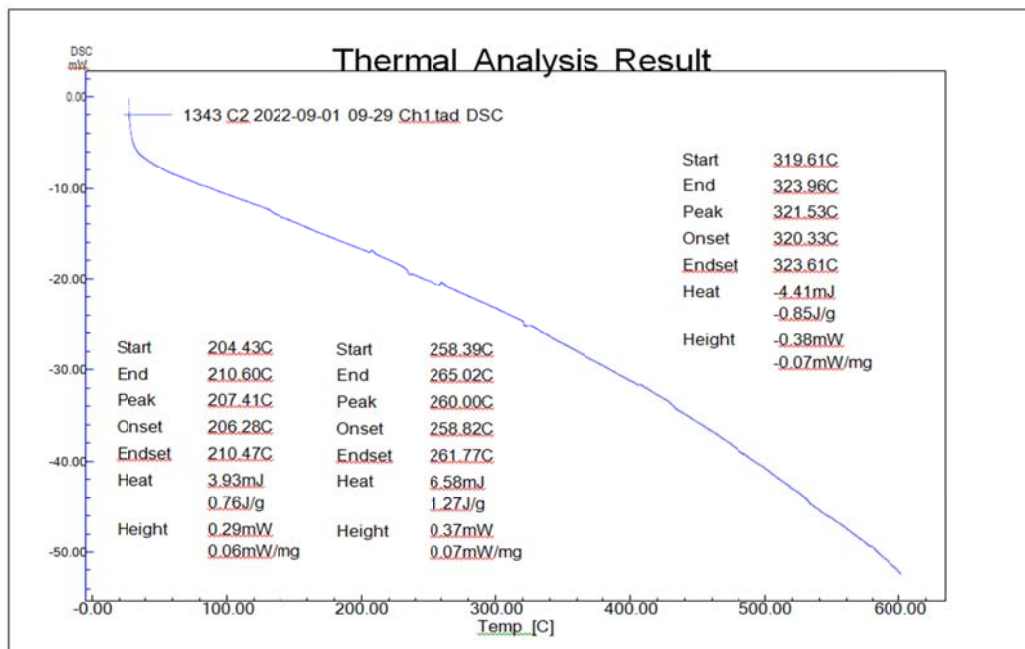


1. C2

[File Information]		[Temp Program]	
File Name:	1343 C2 2022-09-01 09-29 Ch1.tad	Start Temp [°C]	30
Sample Name:	C2	Temp Rate [°C/min]	10
Lot No:	1343	Hold Temp [°C]	600
Acquisition Date	2022/09/01	Hold Time [min]	0
Acquisition Time	09:29:32(+0700)	Gas	Nitrogen
Detector:	DSC-60		
Serial No:	C30935200137SA		
Operator:	Heri		
Atmosphere:	Nitrogen		
Flow Rate:	10[ml/min]		
Cell:	Aluminum Crimping		
Sample Weight:	5.190[mg]		
Molecular Weight:	0.00		

[Analysis Result]

[DSC Peak]	1	2	3
Peak			
[°C]	207.41	260.00	321.53
Onset			
[°C]	206.28	258.82	320.33
Endset			
[°C]	210.47	261.77	323.61
Heat			
mJ	3.93	6.58	-4.41
J/g	0.76	1.27	-0.85
Height			
mW	0.29	0.37	-0.38
mW/mg	0.06	0.07	-0.07



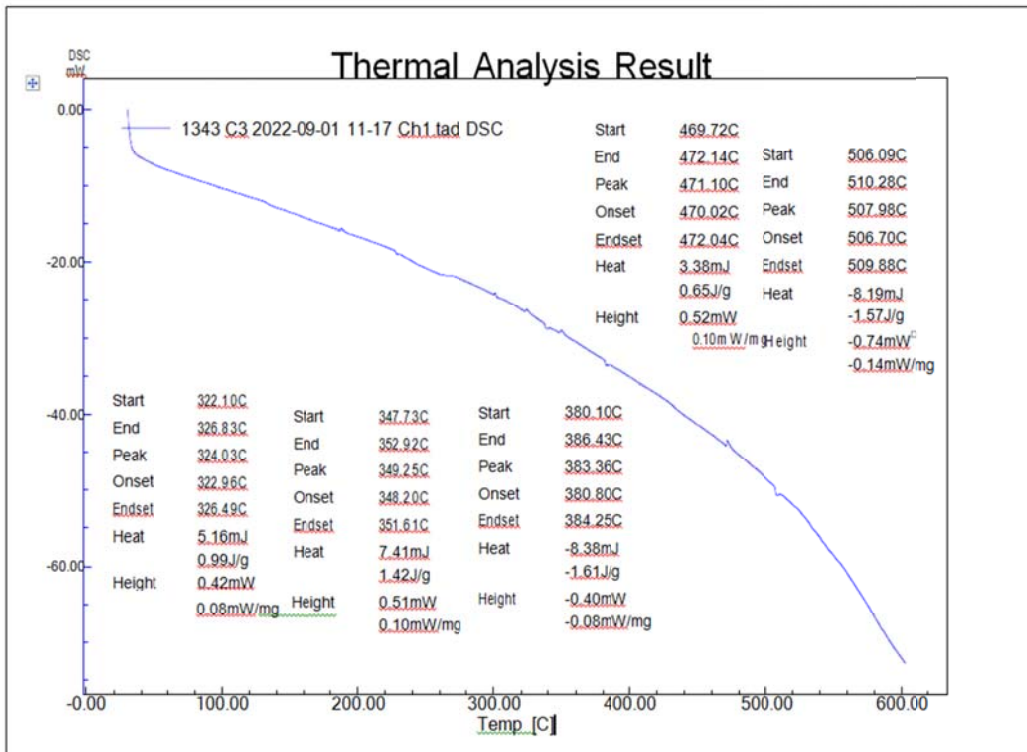
2. C3

[File Information]		[Temp Program]	
File Name:	1343 C3 2022-09-01 11-17 Ch1.tad	Start Temp [°C]	30
Sample Name:	C3	Temp Rate [°C/min]	10
Lot No:	1343	Hold Temp [°C]	600
Acquisition Date	2022/09/01	Hold Time [min]	0
Acquisition Time	11:31:34(+0700)	Gas	Nitrogen
Detector:	DSC-60		
Serial No:	C30935200137SA		
Operator:	Heri		
Atmosphere:	Nitrogen		
Flow Rate:	10[ml/min]		
Cell:	Aluminum Crimping		
Sample Weight:	5.220[mg]		
Molecular Weight:	0.00		






[Analysis Result]

[DSC Peak]	1	2	3	4	5
Peak					
[°C]	324.03	349.25	383.36	471.10	507.98
Onset					
[°C]	322.96	348.20	380.80	470.02	506.70
Endset					
[°C]	326.49	351.61	384.25	472.04	509.88
Heat					
mJ	5.16	7.41	-8.38	3.38	-8.19
J/g	0.99	1.42	-1.61	0.65	-1.57

Height					
mW	0.42	0.51	-0.40	0.52	-0.74
mW/mg	0.08	0.10	-0.08	0.10	-0.14



Experimental Study of Modified Absorber Plate Integrated with Aluminium Foam of Solar Water Heating System

Muhammad Hasan Basri^{*,***} , Jalaluddin ^{**†} , Rustan Tarakka ^{**} , Muhammad Syahid ^{**} ,
M. Anis Ilahi Ramadhani ^{*} 

* Graduate Student in Mechanical Engineering Department, Hasanuddin University, Gowa, 92171, Indonesia

** Department of Mechanical Engineering, Hasanuddin University, Gowa, 92171, Indonesia

*** Department of Mechanical Engineering, Tadulako University, Palu, 94118, Indonesia

(muhasanbasri77@gmail.com, jalaluddin_had@yahoo.com, rustan_tarakka@yahoo.com, syahid.arsjad@gmail.com, muhammad.anis09@gmail.com)

† Corresponding Author; Jalaluddin, Department of Mechanical Engineering, Hasanuddin University, Gowa, 92171, Indonesia,
Tel: +62411 586015, Fax: +62411 586015, jalaluddin_had@yahoo.com

Received: 04.04.2022 Accepted: 06.05.2022

Abstract- The Solar Water Heating System (SWHS) is a water heater equipment that utilizes solar energy for domestic scale needs. The potential generated by this system can reduce the energy demand of the building sector, reduce peak demand for electricity, and reduction in pollution. This study aims to analyze the performance of SWHS experimentally by modifying the addition of aluminium foam material at the bottom of the absorber plate and the top of the absorber plate. The absorber plate models are Standard Flat-Plate (SFP), SFP with Bottom Aluminium Foam (SFP-BAF), and SFP with Top Aluminium Foam (SFP-TAF). The experimental study was carried out for the three models under similar conditions using a Solar Thermal Energy Unit. The effect of flowrate variations and slope angles were also investigated. The study results show that the SFP-BAF model with the angle of 30° achieved the highest efficiency of 88.4%, 86.9%, and 83.9% at a flow rate of 8 L/h, 10 L/h, and 12 L/h, respectively. The benefits of adding aluminium foam to the absorber plate is to increase the absorption of radiant heat energy transmitted from the absorber plate, the storage time of thermal energy, and the thermal efficiency of the collector.

Keywords Solar water heating system; absorber flat-plate; aluminium foam; efficiency.

1. Introduction

The Solar Water Heating System (SWHS) is a water heater equipment that utilizes solar energy for domestic scale needs. The potential generated by this system can reduce the energy demand of the building sector, and peak demand for electricity [1]. Renewable energy sources can be combined with conventional energy sources or energy storage systems [2], as well as smart control element heating minimizes energy cost [3], electricity consumption and pollution [4].

Researchers have worked on a variety of SWHS advances, including changing the shape of the absorber plate, using porous materials, and modifying the transparent cover glass using Fluorine Doped Tin Oxide Nanomaterials [5].

The current development of SWHS is modifying the Flat-Plate Collector (FPC) material. Jalaluddin et al. [6] conducted a study to analyze the thermal efficiency of SWHS using a V-shaped absorber plate. The results showed that the SWHS using a V-shaped absorber plate had an efficiency of 3.6-4.4 % against systems that use standard plates. Further research by Jalaluddin et al. [7], adding phase change material (PCM) to the V-shaped SWHS is increased the average efficiency significantly of 20%, 14% and 13% with flowrates of 0.5; 1 and 1.5 L/min respectively. However, this design has disadvantage due to fluid leakage.

Another development of FPC is by adding porous materials such as asphalt material, aluminium foam and copper foam. Pukdum et al. [8] investigated the performance

of SWHS using asphalt material as an absorber plate. The results showed that the maximum absorber plate temperature was 60 °C, the difference between the water inlet and outlet temperature was 17.2 °C, and the efficiency of SWHS is in the range of 70-79%. Then, Guerroudj and Kahalerras [9] investigated the effect of the design of the shape (rectangular, triangular) and structure of metal foam blocks on collectors. The results show that the square foam block shape is more optimal at high Darcy Number and Reynold Number parameters, resulting in a higher heat transfer rate. In addition, Chen and Huang [10] studied the aluminium foam block parallel under the absorber plate with a certain thickness. This study shows that inserting metal foam blocks at the inner wall of the absorber is an effective method for improving the thermal performance of flat-plate solar water collectors.

Another approach is carried out by Valizade et al. [11] with arrangement a block of copper foam at a certain distance inside the tube on the parabolic collector. The arrangement of the copper foam block increases the thermal efficiency of the collector significantly compared to without the use of the foam block. In addition to developing foam blocks, some researchers use full-filled metal foam in the collector. For steam production, a parabolic trough collector is used since it can produce high temperatures (100-400° C) [12]. In, addition, Baig and Ali [13] used aluminium foam and paraffin blocks in the double pass solar air heater model. The results show that when outside air temperature is maintained between 15-29°C, the four ducts embedded with aluminum foam and paraffin wax without fan obtain maximum efficiency about 97 %.

Saedoddin et al. [14] used full-filled copper foam affixed under the absorber and insulator plates at a 45° angle. The study results showed an increase in absorption heat energy reaching 18.5%, and the Nusselt number increased by 82% compared to the foam material. In addition, the value of the thermal efficiency of the collector also increases with a given flow rate variation. Using metal foam in a filled form was also developed by Anirudh and Dhinarkhan [15]. Simulation analysis through radiation modelling and the Rosseland approach to the inclination angle. The modelling analysis results in the maximum performance occurring at a slope between 15° and 30°, but an increase in the inclination angle more 30° will reduce the efficiency.

In this paper, studies on the use of full-filled aluminium foam at the bottom of the absorber plate have been done by some researchers, but studies of full-filled aluminium foam placed on the top of the absorber plate are still not investigated by researchers as a heat storage material. Based on in this, the full-filled aluminium foam placed on the bottom and the top of the absorber plate was used with the variation on the collector tilt angle and fluid flow rate to evaluate the collector's performance. Therefore, this study aims to analyze the performance of SWHS experimentally by modifying the addition of full-filled aluminium foam material at the bottom and the top of the absorber plate.

2. Experimental Set-up and Description

This research was conducted at the Renewable Energy Laboratory, Mechanical Engineering of Hasanuddin University, Gowa campus (1190 30' 06.1" BT and 050 13' 52.4" LS). As shown in Fig. 1 and its specification shown in Table 1, a solar thermal energy unit is used to investigate the thermal performance of the absorber plate. The equipment is equipped with its lighting unit, a flat-plate collector that absorbs radiation energy and transfers heat to water. Water is circulated through a storage reservoir using a water pump. The reservoir tank has in and out channels for tap water, and heat can be removed if necessary. The water content of the tank can also be heated with integrated heating. The flow rate is controlled via the flow rate potentiometer switch, corresponding to the pump rotation speed. The equipment is also equipped with sensors to detect temperature, lighting, and flow rate.

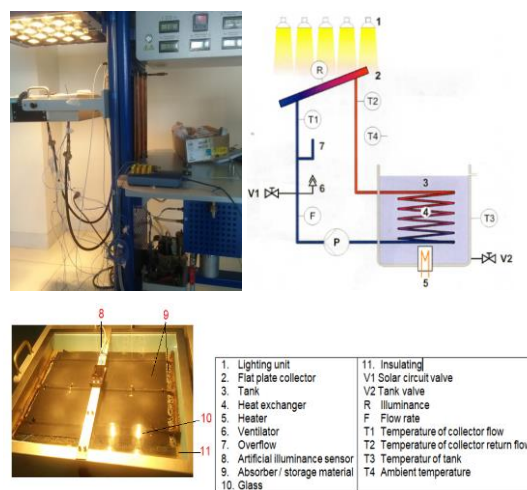


Fig. 1. ET 202 solar thermal energy unit

Table 1. Solar thermal energy unit specifications

Description	Dimension	Unit
<i>ET 202 FPC</i>		
Absorbing surface	320 x 340	mm
Angle adjustment	0-60	deg
Height adjustment	532	mm
<i>Lighting unit</i>		
Halogen lighting units	25 x 50	W
Illuminance	0,5 – 2,5	kW/m ²
<i>Peristaltic Pump</i>		
Variable Flow rate	3 – 20	L/h
<i>Measuring range</i>		
Temperature	0 – 100	°C
Flow rate	0 – 30	L/h
Irradiance	0 – 3	kW/m ²

The test section is a rectangular box with absorber plates and storage materials. In this test, three (3) models of plate absorber such as 1) Standard Flat-Plate (SFP); 2) SFP with Bottom Aluminium Foam (SFP-BAF), and 3) SFP with Top Aluminium Foam (SFP-TAF). The three (3) plate absorber models are presented in Fig. 2. Table 2 shows the

specifications of the absorbent plate model. Experimental testing of each absorber model using a thermal storage unit under the same conditions for 2 hours. Record data of all parameters are recorded automatically at 1-minute intervals. The recorded data are included artificial solar intensity, inlet and outlet fluid temperatures, and flow rate. The recorded measurements and performance analysis while experimenting is made easier thanks to the ET 202 software [16].

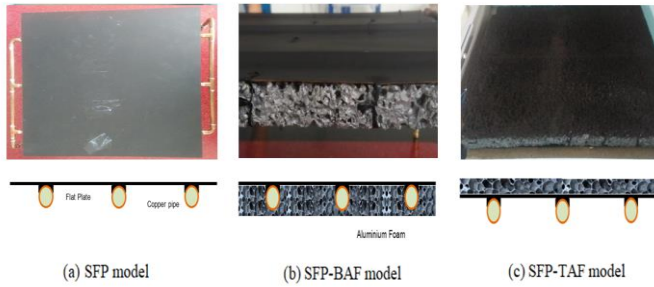


Fig. 2. Collector models

Table 2. Absorber plate specifications

Description FPC	Dimension	Unit
Absorbing plate surface	0,285 x 0,300 x 0,002	m
Pipe diameter	0,008	m
Flow channel cross section	$5,02 \times 10^{-5}$	m ²
Aluminium foam	0,285 x 0,300 x 0,15	m
Flow rate	8, 10, 12	L/h

3. Thermal Performance

In steady state, the performance of a solar collector is described by an energy balance that indicates the distribution of incident solar energy into useful energy gain, thermal losses, and optical losses. The useful energy output of a collector of area A_c is the difference between the absorbed solar radiation and the thermal loss [17]:

$$Q_u = A_c [S - U_L (T_{pm} - T_a)] \tag{1}$$

Q_u , the valuable energy is also calculated based on the temperature measurement data of the inlet and outlet water of the collector specified in equation 2 [18].

$$Q_u = \int Q_u dt = \dot{m} C_p (T_o - T_i) \tag{2}$$

Where m is the mass flow rate (kg/s), C_p is the specific heat (kJ/kg.K) and T_o is the temperature of the fluid leaving the collector (°C), and T_i is the temperature of the fluid entering the collector (°C).

The collector's efficiency is the ratio of the useful gain over some specified time period to the incident solar energy over the same time period [18].

$$\eta = \frac{\int Q_u dt}{A_c \int I_T dt} \tag{3}$$

I_T is the solar intensity (W/m^2), and A_c is the collector surface area (m^2).

4. Results and Discussion

4.1. Solar Intensity

The intensity of solar radiation on the test equipment comes from lighting units measured from an artificial solarimeter. Fig. 5 shows the solar radiation intensity from the three models including SFP, SFP-BAF and SFP-TAF at a tilt of 0° and 10 L/h. Such models tend to be the same solar intensity values about 1.3 – 1.4 kW/m² for 1-hour operation.

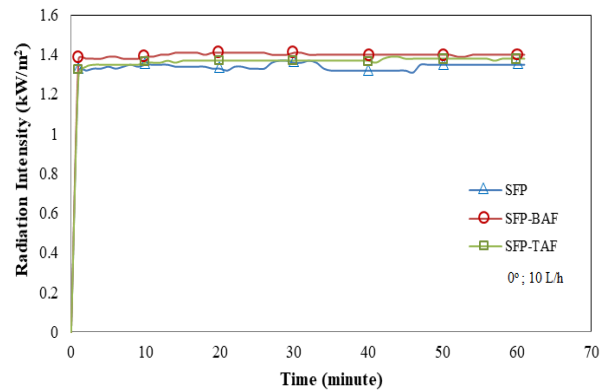


Fig. 5. Radiation intensity based on position

Changes in the angle of inclination on SFP-BAF model is shown in Fig. 6. The angular position of the collector determines the amount of radiation intensity that reaches the glass absorber plate, the reflection of radiation back to the glass and the level of absorptivity of the absorber plate. The maximum radiation intensity is achieved at 0° angle of 1.4 kW/m² and the minimum is 30° angle of 1.16 kW/m². This study is in accordance with the results of research conducted by Taheri et al. [19] that an increase in the angle of inclination causes the transmissivity with absorptivity to decrease.

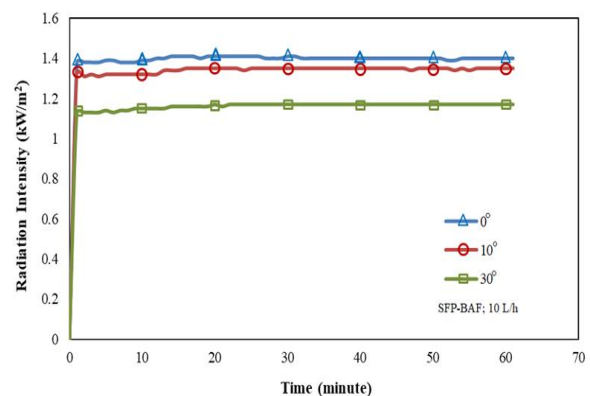


Fig. 6. Radiation intensity based on the tilt angle

Fig.7 shows correlation between flow rate and radiation intensity. It shows that the radiation intensity for all models tends to constant on the flow rate change. Water flow rates of

8 L/h, 10 L/h, and 12 L/h with radiation intensity is approximately 1.3 – 1.4 kW/m².

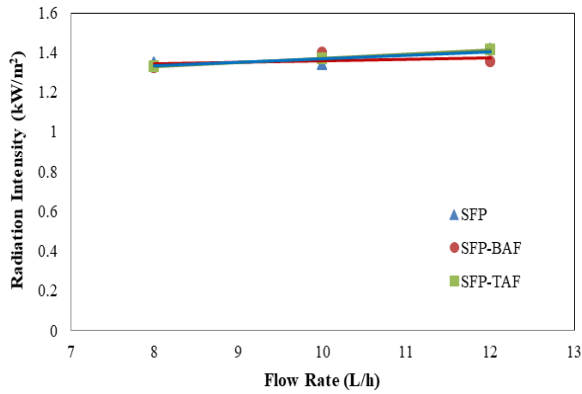


Fig. 7. Radiation intensity based on flow rate

4.2. Inlet and Outlet Water Temperatures

Fig. 8 shows the inlet and outlet water temperatures at an angle of 0° and a flow rate of 10 L/h. Inlet water temperature in all models is between 28-29 °C. The SFP-BAF model has a higher outlet water temperature than other models. The maximum outlet water temperature of the SFP-BAF model is around 46.3 °C for 1 hour. After the heat lighting units are stopped, the temperature of the water inlet and outlet reaches the same temperature at a certain time. The heat stored in the SFP-BAF and SFP-TAF model has a longer storage time than the standard model (SFP). The SFP-TAF and SFP BAF models have a duration time of approximately 30 minutes. The addition of aluminium foam at the bottom of the absorber plate (SFP BAF model) is beneficial in storage heat. This study is in accordance with the results obtained by Prasanth et al. [20] that the fluid temperature increases 2–2.5 times after passing through the heat energy storage material.

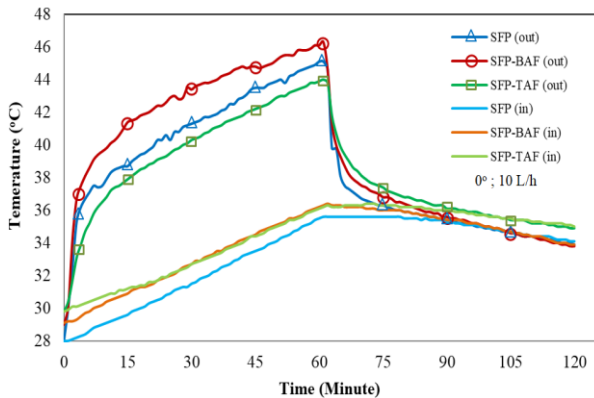


Fig. 8. Water inlet and outlet temperatures based on position models

Fig. 9 shows the inlet and outlet water temperatures at model SFP-BAF at a flow rate of 10 L/h with various inclination angles. The highest outlet water temperature is obtained at an angle of 10° around 47.3 °C, and the lowest is 30° around 45.5 °C. The change in inclination angles from 0 to 30°, causes the heat absorption by the absorber plate to water reduced. After the heat lighting units are stopped, the outlet water temperature at an angle of 10° is still maintained

for 30 minutes. The aluminium foam at the bottom of the absorber plate effectively retains the heat. However, all stored heat is not overall transferred to the circulating fluid. The heat stored in the aluminium foam may be dissipated to the environment. This may be caused by the high dimension difference between the thickness of the aluminium foam and the diameter of the pipe which induces heat to move to the bottom away. The large specific area of the metal foam provides higher heat transfer fluid mixing, heat transfer rates, and thermal performances [10].

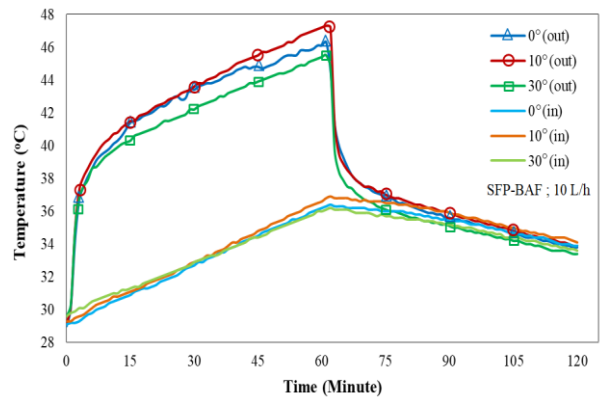


Fig. 9. Water inlet and outlet water temperatures based on tilt angle

Fig. 10 shows the water temperatures of the collector concerning the change in flow rate. All models have the same trend of decreasing the outlet water temperature if the flow rate increases. The SFP-BAF model obtains the maximum outlet temperature value for all flow rates. 8 L/h flow rate has the heat transfer from the absorber plate surface to the fluid is higher than other flow rate. It reaches 47.9 °C. In addition, the addition of aluminium foam also contributes to the effect of transferring heat to the fluid so that the outlet temperature is also high.

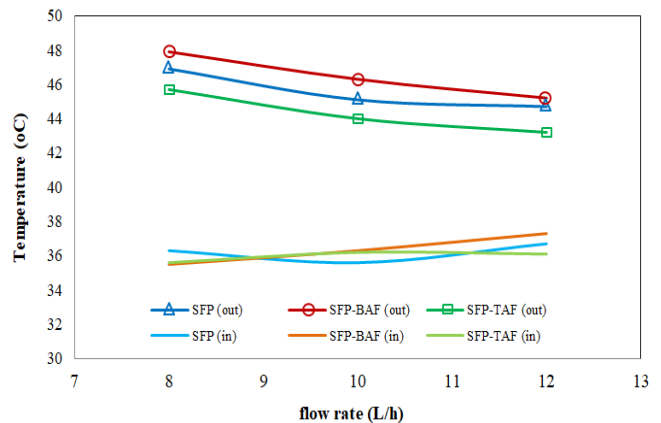


Fig. 10. Inlet and outlet water temperature based on flow rate

4.3. Collector Efficiency

Fig. 11 shows correlation between the thermal efficiency and operation time. In the first 1 hour period, the thermal efficiency reaches the constant after around 20 minutes operation with around 80 percent of efficiency. After 1 hour period, the thermal efficiency of the collector is zero because the intensity radiation is turned off. However, the heat is still

stored in aluminium foam although the intensity radiation is turned off. In addition, the efficiency value tends to decrease along with the increase in the circulating water flow rate. At a flow rate of 10 L/h, the SFP-BAF model is higher efficiency than the other two models. The addition of aluminium foam at the bottom significantly helps absorb heat, store, and retain heat. For increasing the time of heat storage, the specific treatment of aluminium foam needs to modify with reducing the thickness of the aluminium foam.

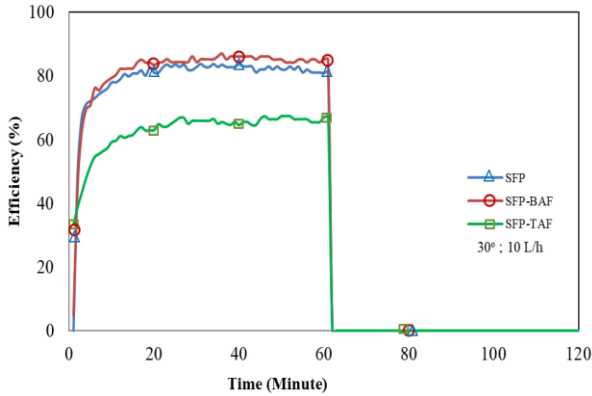


Fig. 11. Collector efficiency based on position models

Fig. 12 shows the efficiency comparison of the slope angle of the SFP-BAF model at a flow rate of 10 L/h. It can be seen that the greater the angle of inclination, the greater the efficiency of the collector. The SFP-BAF model has a maximum thermal efficiency value at an angle of 30° by 86.9% at a flow rate of 10 L/h. The lowest efficiency is obtained at an angle of 0° degrees. The addition of the angle of inclination causes to decrease the radiation intensity consequently reducing the thermal efficiency of the collector. Although collectors' performance with porous materials increases with increasing inclination angle, maximum performance is obtained at intermediate angle, whereas every further increase angle decreases performance [14].

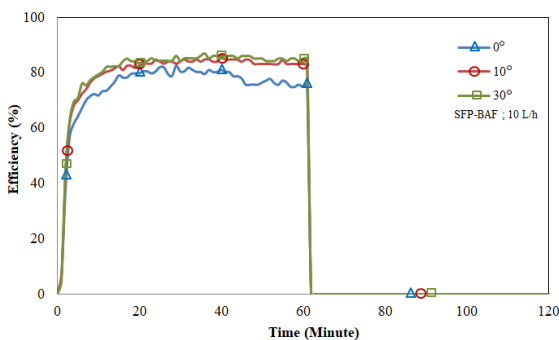


Fig. 12. Collector efficiency SFP-BAF models based on tilt angles

Fig. 13 shows the correlation between the thermal efficiency and flow rate at an angle of 30°. The collector efficiency of the three models tends to decrease with increasing the flow rate. The SFP-BAF model achieved the highest efficiency of 88.4% at a rate of 8 L/h. For flow rates of 10 L/h and 12 L/h, the SFP-BAF model has also the highest efficiency of 86.9% and 83.9%, respectively. The high-efficiency value is due to the low radiation intensity

absorbed by the aluminium foam, but the heat transferred to the fluid is high. The efficiency of the SFP-TAF model tends to constant value of around 70-80%.

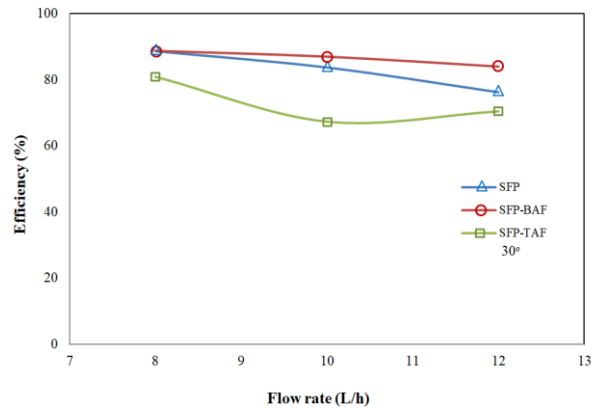


Fig. 13. Comparison collector efficiency based on flow rate

The placement of aluminium foam in the collector can act as an absorber and heat storage. The aluminium foam placed at the bottom of the absorber plate functions more as a heat storage material because it can help increase the water output temperature and retain heat for a particular time. Then, the benefits of adding aluminium foam to the absorber plate is to increase the storage time of thermal energy, and the thermal efficiency of the collector. In contrast, the placement of aluminium foam at the top functions more as a good heat absorber because it can increase the level of heat absorption of the collector.

4.4. Uncertainty analysis

Uncertainty is defined as the imperfection of multiple measuring elements. Uncertainty is caused by a variety of factors, including measurement methods, measuring instruments, operators, and the surrounding environment. The uncertainty analysis is required to assess the correctness of the measure's outcomes. As a result, the data's validity is verified, and a detailed approach for calculating accurate and complete uncertainty is proposed. As shown in Equation (4), the uncertainties that arise as a result of computing (U_R) owing to multiple independent variables.

$$U_R = \left[\left(\frac{\partial R}{\partial x_1} u_1 \right)^2 + \left(\frac{\partial R}{\partial x_2} u_2 \right)^2 + \dots + \left(\frac{\partial R}{\partial x_n} u_n \right)^2 \right]^{1/2} \quad (4)$$

Where the result R is a function in terms of its independent variables as x_1, x_2, \dots, x_n , thus $R = R(x_1, x_2, \dots, x_n)$, u_1, u_2, \dots, u_n are the uncertainties in the independent variables and U_R is the uncertainty of the result.

The temperature of the water inlet, outlet, and flow rate were measured in this investigation using the previously described equipment. Equation (5) is used to determine and quantify the uncertainties of each estimated and measured parameter. The following is how the uncertainty in the temperature of the water inlet, outlet, and flow rate can be calculated [8].

$$Q = f(\dot{m}, C_p, T_i, T_o) \quad (5)$$

$$U_R = \left[\left(\frac{\partial Q}{\partial \dot{m}} u_{\dot{m}} \right)^2 + \left(\frac{\partial Q}{\partial C_p} u_{C_p} \right)^2 + \left(\frac{\partial Q}{\partial T_i} u_{T_i} \right)^2 + \left(\frac{\partial Q}{\partial T_o} u_{T_o} \right)^2 \right]^{1/2} \quad (6)$$

using algebraic manipulation, we were able to acquire

$$\frac{U_Q}{Q} = \left[\left(\frac{U_{\dot{m}}}{\dot{m}} \right)^2 + \left(\frac{U_{C_p}}{C_p} \right)^2 + \left(\frac{U_{T_o}}{T_o - T_i} \right)^2 + \left(\frac{U_{T_i}}{T_o - T_i} \right)^2 \right]^{1/2} \quad (7)$$

Total measurement errors are estimated to be $\pm 0.171\%$ for inlet water temperature and $\pm 0.172\%$ for outlet water temperature. The measured values can be used to compute the mass flow rate. The overall accuracy of the mass flow rate is $\pm 2.4\%$, according to the data.

5. Conclusions

Thermal performances of SWHS by using of full-filled aluminium foam at the bottom and the top of the absorber plate was investigated. The results presented of water outlet and inlet temperature, and thermal efficiency. Based on position, SFP-BAF model have a higher outlet water temperature than the other model around $46.3\text{ }^\circ\text{C}$ at inclination angle 0° and 10 L/h flow rate. Then, based on inclination angle on SFP-BAF, the maximum water outlet temperature have value approximately $47.3\text{ }^\circ\text{C}$ at angle 10° . Lastly, the SFP-BAF model with angle of 30° achieved the highest efficiency of 88.4% , 86.9% , and 83.9% at a flow rate of 8 L/h , 10 L/h , and 12 L/h , respectively.

The benefits of adding aluminium foam to the absorber plate is to increase the absorption of radiant heat energy transmitted from the absorber plate, the storage time of thermal energy, and the thermal efficiency of the collector.

Acknowledgements

This study was supported by the Laboratory-Based Education (LBE) Research Fund 2021, Engineering Faculty of Hasanuddin University.

References

[1] A. Rout, S. S. Sahoo, S. Thomas, and S. M. Varghese, "Development of Customized Formulae for Feasibility and Break-Even Analysis of Domestic Solar Water Heater," *International Journal of Renewable Energy Research*, vol. 7, no. 1, pp. 386–398, 2017.

[2] A. Colak and K. Ahmed, "A Brief Review on Capacity Sizing, Control and Energy Management in Hybrid Renewable Energy Systems," *2021 10th International Conference on Renewable Energy Research and Application (ICRERA)*, pp. 453–458, 2021.

[3] S. Walgama, U. Hasinthara, A. Herath, K. Daranagama and S. Kumarawadu, "An Optimal Electrical Energy Management Scheme for Future Smart Homes," *2020*

IEEE 8th International Conference on Smart Energy Grid Engineering (SEGE), pp. 137–141, 2020.

[4] H. Lill, A. Allik, M. Hovi, K. Loite and A. Annuk, "Integrated Smart Heating System in Historic Buildings," *2019 7th International Conference on Smart Grid (icSmartGrid)*, pp. 92–96, 2019.

[5] V. Msomi and O. Nemraoui, "Improvement of the performance of solar water heater based on nanotechnology," *2017 IEEE 6th International Conference on Renewable Energy Research and Applications (ICRERA)*, pp. 524–527, 2017.

[6] Jalaluddin, A. Effendy, and R. Tarakka, "Experimental Study of an SWH System with V-Shaped Plate," *J. Eng. Technol. Sci.*, vol. 48, no. 2, pp. 207–217, 2016.

[7] Jalaluddin, R. Tarakka, M. Rusman, and A. A. Mochtar, "Performance Investigation of Solar Water Heating System with V-Shaped Absorber Plate Integrated PCM Storage," *International Journal on Engineering Applications (IREA)*, vol. 8(5), 2020.

[8] J. Pukdum, T. Phengpom, and K. Sudasna, "Thermal Performance of Mixed Asphalt Solar Water Heater," *International Journal of Renewable Energy Research*, vol. 9, no. 2, pp. 712–720, 2019.

[9] N. Guerroudj and H. Kahalerras, "Mixed convection in a channel provided with heated porous blocks of various shapes," *Energy Conversion and Management*, vol. 51, pp. 505–517, 2010.

[10] C. C. Chen and P. C. Huang, "Numerical study of heat transfer enhancement for a novel flat-plate solar water collector using metal-foam blocks," *International Journal of Heat and Mass Transfer*, vol. 55, no. 23–24, pp. 6734–6756, 2012.

[11] M. Valizade, M. M. Heyhat, and M. Maerefat, "Experimental study of the thermal behavior of direct absorption parabolic trough collector by applying copper metal foam as volumetric solar absorption," *Renewable Energy*, vol. 145, pp. 261–269, 2020.

[12] M. E. Shayan, G. Najafi, and F. Ghasemzadeh, "Advanced Study of the Parabolic Trough Collector Using Aluminum (III) Oxide," *International Journal of Smart Grid*, vol. 4, pp. 111–116, 2020.

[13] W. Baig and H. M. Ali, "An experimental investigation of performance of a double pass solar air heater with foam aluminum thermal storage medium," *Case Studies in Thermal Engineering*, vol. 14, p. 100440, 2019.

[14] S. Saedodin, S. A. H. Zamzamin, M. E. Nimvari, S. Wongwises, and H. J. Jouybari, "Performance evaluation of a flat-plate solar collector filled with

- porous metal foam: Experimental and numerical analysis,” *Energy Conversion and Management*, vol. 153, pp. 278–287, 2017.
- [15] K. Anirudh and S. Dhinakaran, “Numerical study on performance improvement of a flat-plate solar collector filled with porous foam,” *Renewable Energy*, vol. 147, pp. 1704–1717, 2020.
- [16] K. Boedecker and J. Rohweder, *Experiment Instructions: ET 202 Principles of Solar Thermal Energy*. Germany: Gunt Hamburg, 2015.
- [17] J. A. Duffie (Deceased), W. A. Beckman, and N. Blair, *Solar Engineering of Thermal Processes, Photovoltaics and Wind*, 1st ed. Wiley, 2020.
- [18] N. Roonprasang, P. Namprakai, and N. Pratinthong, “Experimental studies of a new solar water heater system using a solar water pump,” *Energy*, vol. 33, no. 4, pp. 639–646, 2008.
- [19] Y. Taheri, K. Alimardani, and B. M. Ziapour, “Study of thermal effects and optical properties of an innovative absorber in integrated collector storage solar water heater,” *Heat and Mass Transfer*, vol. 51, pp. 1403–1411, 2015.
- [20] N. Prasanth, M. Sharma, R. N. Yadav, and P. Jain, “Designing of latent heat thermal energy storage systems using metal porous structures for storing solar energy,” *Journal of Energy Storage*, vol. 32, p. 101990, 2020.

Study of Modified Absorber Plate with Aluminium Foam of Solar Water Heating System

MUHAMMAD Hasan Basri^{1,a}, JALALUDDIN^{2,b*}, RUSTAN Tarakka^{2,c},
MUHAMMAD Syahid^{2,d} and M.ANIS Ilahi Ramadhani^{1,e}

¹Graduate Student in Mechanical Engineering Department, Hasanuddin University, Jl. Poros Malino KM. 6 Bontomarannu Gowa, 92171, Indonesia

²Department of Mechanical Engineering, Hasanuddin University, Jl. Poros Malino KM. 6 Bontomarannu Gowa, 92171, Indonesia

^amuhhasanbasri77@gmail.com, ^{b,*}jalaluddin_had@yahoo.com, ^csyahid.arsjad@gmail.com,
^drustan_tarakka@yahoo.com, ^emuhammad.anis09@gmail.com

Keywords: Solar Water Heater System, Aluminium Foam, Absorber Plate.

Abstract. Solar water heating system (SWHS) is water heating equipment that utilizes solar energy for domestic and industrial needs. An absorber plate is the main part of the SWHS that functions to absorb solar energy. Porous materials are efficient in increasing heat transfer, energy efficiency, energy storage, and reducing reflectance losses. Efforts have been made to add aluminium foam as a porous material on the lower and upper surfaces of the absorber plate. Porous materials function absorbs heat and store radiant heat energy before being transferred to the fluid. Experimental tests were carried out by testing three models of absorber plates on a solar thermal energy unit with similar conditions. The first model is a standard flat plate (SFP) without aluminium foam. The second model combines standard flat plate and aluminium foam (SFP-TAF), placed on top of the SFP. The third model combines standard flat plate and aluminium foam (SFP-BAF), placed under the SFP. The results showed that the SFP-BAF model has a higher thermal efficiency than the other models. The SFP-BAF model has an efficiency increase of 2.71 % at a flow rate of 10 L/h and 5.39 % flow rate of 12 L/h compared with the standard model (SFP). The position of the aluminium foam at the bottom surface is substantial enough to help absorb and store radiant heat for transfer to circulating water.

Introduction

The priority of energy policy is the utilization of renewable energy sources such as solar energy. Solar energy is used in industrial and domestic applications for water heating, water distillation, space heating, etc. The solar water heating system (SWHS) design is built-in lower operating temperatures, fewer mechanical components, and is easy to fabricate. However, the performance of the SWHS is still inadequate compared to conventional devices due to the working fluid's low operational heat transfer characteristics [1]. Recent developments in the thermo-economic performance of the SWHS include collector design, modification of the thermo-physical properties of heat transfer fluids, integrated thermal energy storage, and flat plate solar collector (FPSC) hybrid systems.

The increase in the design factor and the convective heat transfer coefficient between the fluid and the absorber material is the most desirable factor to improve the overall performance of the solar collector. Porous materials are efficient in increasing heat transfer, energy efficiency, energy storage [2], and reflectance losses [3]. The use of porous materials affects the thermal efficiency of the system, such as black steel wool fibres porous in solar still [4], aluminium foam in solar air heater [5], and copper foam in volumetric solar absorption [6].

Several researchers have studied the advantages of adding porous materials to engineering applications. The addition of absorbent material with a low volume capacity can increase higher temperatures which have a direct effect on increasing energy storage in the solar pond [7], an increase in temperature of 2-2.5 times from the initial temperature after passing through a thermal

energy storage system designed from the structure metal foam and PCM [8]. In addition, the use of porous materials with agitators in solar water heaters can increase convective heat transfer, reduce thermal losses, and increase efficiency gradually [9]. The development of porous material (metal foam) in the SFP collector, especially the placement of metal foam at the bottom of the absorber plate, began to be developed. The insertion of metal foam between the absorber plate and the insulator indicates an increase in heat transfer to the collector and the thermal efficiency of the collector [10]. Combining metal foam block and PCM on the collector increases the heat transfer coefficient [11].

The development of water heating technology to produce hot water has been studied in the Renewable Energy Laboratory of Hasanuddin University. The possibility of producing hot water using a hybrid system with a ground source cooling system has been investigated [12–14]. The use of a V-shape absorber plate shown an increase in the absorptivity of the absorber plate [15] and integrated with various PCM materials such as paraffin wax [16]. These studies show that using a V-shape absorber plate and PCM storage provided better performance. However, difficulty in construction for PCM storage due to fluid leakage reduces design simplicity. To improve construction simplicity, using porous material as storage energy should be considered. This research focuses on the study of modified absorber plates with aluminium foam for energy storage. Experimental tests were carried out by testing three models of absorber plates on a solar thermal energy unit with similar conditions.

Experimental Set-Up

This research was conducted at the Renewable Energy Laboratory of Hasanuddin University, Indonesia (1190 30' 06.1" BT and 050 13' 52.4" LS). Testing equipment using a solar thermal energy unit as shown in Fig. 1. The experimental set-up can be seen in Fig. 2. The test section is a rectangular box filled with absorber plates and storage materials. There are three (3) absorber modification models tested, namely 1) Standard Flat Plate (SFP) model, 2) SFP model with Bottom Aluminium Foam (SFP-BAF), and 3) SFP model with Top Aluminium Foam (SFP-TAF). Testing was conducted by running the solar energy unit for 2 hours for each model. Recorded data were collected during testing with an interval of 1 minute automatically. The recorded data include artificial solar intensity, inlet and outlet fluid temperatures, and flow rate.

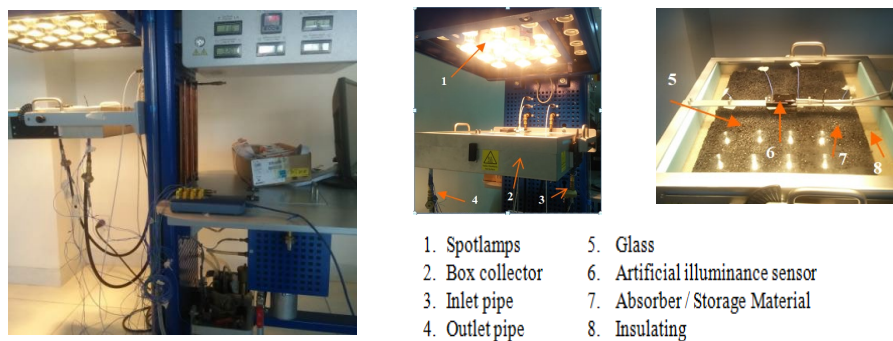


Fig. 1. Solar thermal energy unit

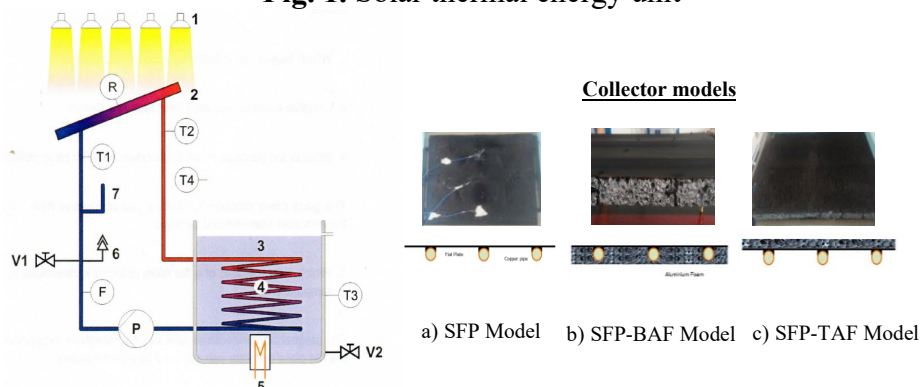


Fig. 2. Experimental set-up

Thermal Performance

The collector's performance is determined by the collector's efficiency, which is obtained from the comparison of the valuable energy of the collector through heating water and available solar energy. Q_u , the useful energy is calculated based on the temperature measurement data of the inlet and outlet water of the collector specified as following

$$Q_u = \dot{m} C_p (T_{f,o} - T_{f,i}) \quad (1)$$

\dot{m} is the mass flow rate (kg/s), C_p is the specific heat (kJ/kg.K) and $T_{f,o}$ is the temperature of the fluid leaving the collector ($^{\circ}\text{C}$), and $T_{f,i}$ is the temperature of the fluid entering the collector ($^{\circ}\text{C}$).

The collector efficiency is as following

$$\eta = \frac{Q_u}{I_T A_C} \quad (2)$$

I_T is the solar intensity (W/m^2), and A_C is the collector surface area (m^2).

Results and Discussion

Experimental tests were carried out by testing for each model of absorber plate on the solar thermal energy unit with similar conditions. The testing was operated with heat source ON in 1 hour and OFF in 1 hour. Recorded data were collected automatically within 2 hours. Fig. 3 shows the radiation intensity in the testing for each model at various fluid flow rates of 10 L/h and 12 L/h. The radiation intensity given by the heat source and received by the absorber plate tends to be constant over time when the heat source is set ON. After the heat source is set OFF, the radiation intensity become zero. The radiation intensity of the models tends to be similar approximately 1.3-1.4 kW/m^2 in the flow rate of 10 L/h. In the flow rate of 12 L/h, the radiation intensity of the SFP and SFP-TAF models is approximately 1.4 kW/m^2 . The radiation intensity of the SFP-BAF model is approximately 1.3 kW/m^2 .

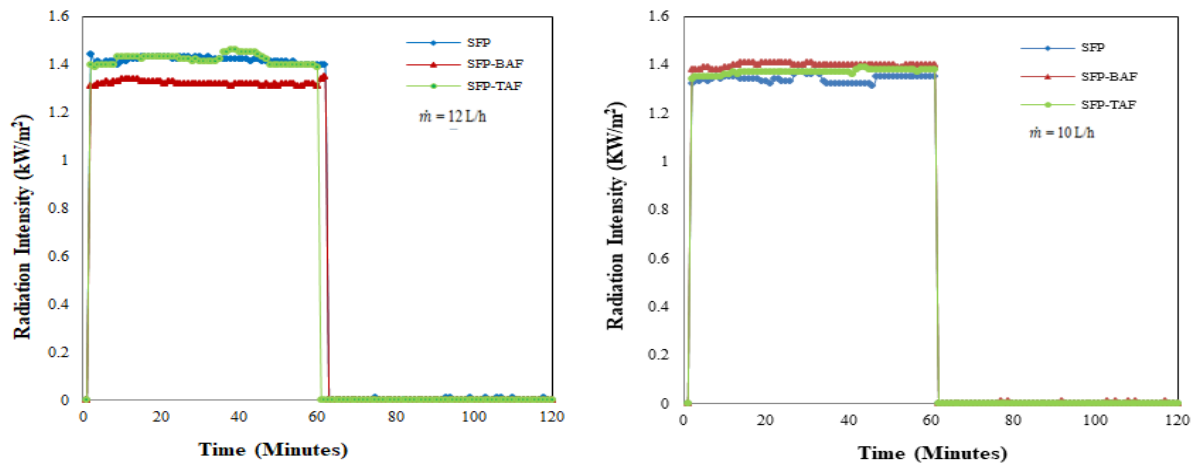


Fig. 3. Radiation intensity

Fig. 4 shows the relationship between the water inlet and outlet temperatures of each testing model. Circulated water flows through the storage tank with closed system. The water inlet temperature has an increasing trend as the water temperature in the storage tank increases. Radiation heat transfer from the absorber plate and storage material to the fluid will continue to increase as long as the heat source is working. After the heat source is stopped, the heat stored in the plate and storage material will slowly decrease until the inlet and outlet water temperatures are the same. The SFP-BAF model tends to have a higher outlet temperature than the other models. The addition of aluminium foam at the bottom as a storage material significantly increases the heat

absorption process from the absorber plate and the heat storage time. However, the influence of fluid flow velocity also affects the increase of the outlet water temperature. If the fluid velocity increases, the outlet temperature will continue to decrease.

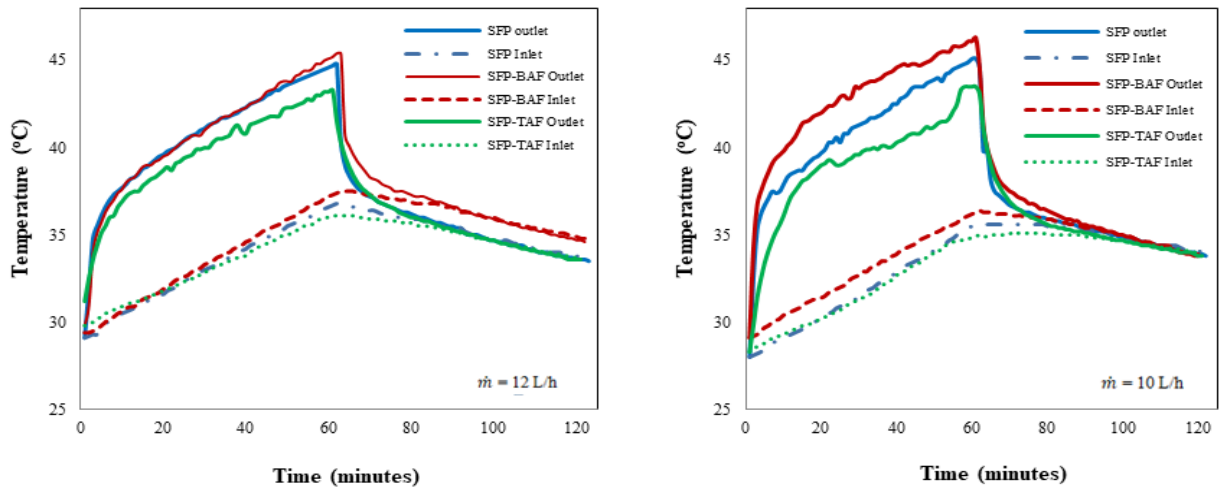


Fig. 4. Water temperature inlet and an outlet collector

Fig. 5. shows the surface temperature of the absorber plate and aluminium foam. The surface temperature of absorber plate and aluminium foam are measured from the amount of radiation absorbed by the upper surface and transmitted to the lower material. The SFP-TAF model has a higher temperature trend than the other models. The average surface temperature is above 90 °C, both at the flow rate of 10 L/h and 12 L/h.

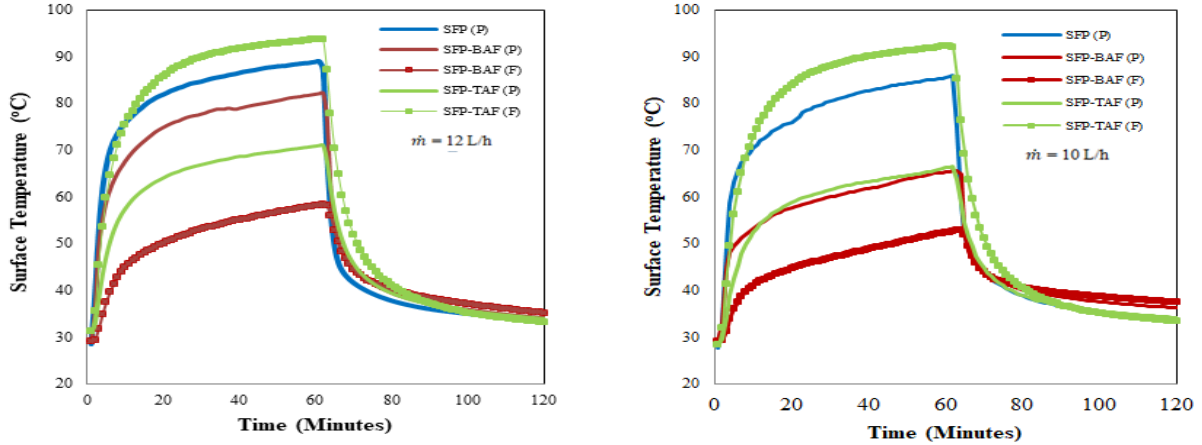


Fig. 5. The surface temperature of the absorber plate and aluminium foam

The placement of aluminium foam at the top in this model indicates a higher heat absorption than the flat plate. The presence of pores in the aluminium foam reduces reflected radiation, thereby increasing the absorption of radiant heat. Thus, the surface temperature of the aluminium foam increases. In the SFB-BAF model, the surface temperature of absorber plate indicates a lower temperature than other models. Its because of transferring energy to the aluminium Foam as an energy storage flaced under the absorber plate.

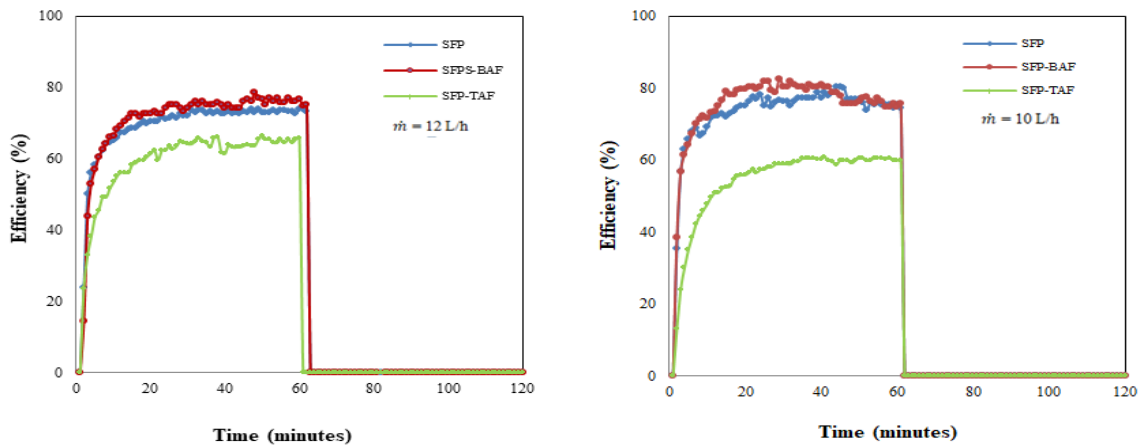


Fig. 6. Thermal efficiency of the collector

Fig. 6. shows the thermal efficiency of the three models of absorber plates. The higher thermal efficiency was obtained in the SFP-BAF model at a flow rate of 10 L/h of 82.5 % as shown in Table 1. The SFP-BAF model has higher thermal efficiency than the SFP and SFP-TAF models in various flow rates. The SFP-BAF model where aluminium foam placed under the absorber plate increased thermal efficiency compared to the standard model (SFP) at the flow rate of 10 L/h and 12 L/h of 2.71% and 5.93 % respectively. The increase of its efficiency is because the aluminium foam acts as a heat-absorbing material and increases heat transfer. The surface temperature of the aluminium foam and the difference of the inlet and outlet temperatures of the circulating water is relatively high. In addition, aluminium foam also acts as a material for storing heat energy and retaining heat for a long time.

On the other hand, the placement of aluminium foam on the top of the absorber plate can reduce the thermal efficiency of the collector. The amount of heat absorbed by aluminium foam will be transferred into absorber plate and circulating water. This transferring heat is not optimal due to storage energy in the aluminium foam. The temperature difference between the inlet and outlet of circulating water seems low. However, the position of the aluminium foam can assist to reduce the reflectance of radiation to maximize energy absorption.

Changes in the circulating water flow rate from 10 L/h to 12 L/h causes decreased thermal efficiency. Increasing the fluid velocity can reduce the conduction time to transfer thermal heat to the circulating fluid [10]. In addition, the thickness of aluminium foam material as a heat storage material needs to be considered because it dramatically affects heat loss to the surroundings and the pressure drop [17].

Table 1. Percentage increase in efficiency

Model	Flow rate [L/h]	Maximum efficiency [%]
SPF	10	80.26
	12	73.92
SFP-BAF	10	82.50
	12	78.58
SFP-TAF	10	60.63
	12	65.79

Conclusions

The performance of the SWHS with the addition of aluminium foam on the top and bottom surfaces of the absorber plate have been investigated experimentally. The SFP-BAF model has a higher thermal efficiency than other models. The SFP-BAF model has an efficiency increase of 2.71 % at a flow rate of 10 L/h and 5.39 % flow rate of 12 L/h compared with the standard model (SFP).

The position of the aluminium foam at the bottom surface is substantial enough to assist absorb and store radiant heat for transfer to circulating water. The effectiveness of the SFP-BAF model needs to be considered in the future related to the thickness of the aluminium foam to increase the heat transfer rate to the fluid and to reduce heat loss to the surroundings.

Acknowledgement

This study was supported by the Laboratory-Based Education (LBE) Research Fund 2021, Engineering Faculty of Hasanuddin University.

References

- [1] K. Modi, D. Shukla, B. Bhargav, J. Devaganiya, R. Deshle, J. Dhodi, D. Patel, A. Patel, Efficacy of organic and inorganic nanofluid on thermal performance of solar water heating system, *Clean. Eng. Technol.* 1, (2020).
- [2] S. Rashidi, J.A. Esfahani, A. Rashidi, A review on the applications of porous materials in solar energy systems, *Renew. Sustain. Energy Rev.* 73 (2017) 1198–1210.
- [3] S. Du, M.J. Li, Y. He, Z.Y. Li, Experimental and numerical study on the reflectance losses of the porous volumetric solar receiver, *Sol. Energy Mater. Sol. Cells.* 214 (2020) 110558.
- [4] A.R.A. Elbar, H. Hassan, Enhancement of hybrid solar desalination system composed of solar panel and solar still by using porous material and saline water preheating, *Sol. Energy.* 204 (2020) 382–394.
- [5] W. Baig, H.M. Ali, An experimental investigation of performance of a double pass solar air heater with foam aluminum thermal storage medium, *Case Stud. Therm. Eng.* 14 (2019) 100440.
- [6] M. Valizade, M.M. Heyhat, M. Maerefat, Experimental study of the thermal behavior of direct absorption parabolic trough collector by applying copper metal foam as volumetric solar absorption, *Renew. Energy.* 145 (2020) 261–269.
- [7] H. Wang, Q. Wu, Y. Mei, L. Zhang, S. Pang, A study on exergetic performance of using porous media in the salt gradient solar pond, *Appl. Therm. Eng.* 136 (2018) 301–308.
- [8] N. Prasanth, M. Sharma, R.N. Yadav, P. Jain, Designing of latent heat thermal energy storage systems using metal porous structures for storing solar energy, *J. Energy Storage.* 32 (2020) 101990.
- [9] B. Kanimozhi, Y.N. Shinde, S.P. Bedford, K.S. Kanth, S.V. Kumar, Experimental Analysis of Solar Water Heater Using Porous Medium with Agitator, *Mater. Today Proc.* 16 (2019) 1204–1211.
- [10] S. Saedodin, A.A.H. Zamzamin, M.E. Nimvari, S. Wongwises, H.J. Jouybari, Performance evaluation of a flat-plate solar collector filled with porous metal foam: Experimental and numerical analysis, *Energy Convers. Manag.* 153 (2017) 278–287.
- [11] Z. Chen, M. Gu, D. Peng, Heat transfer performance analysis of a solar flat-plate collector with an integrated metal foam porous structure filled with paraffin, *Appl. Therm. Eng.* 30 (2010) 1967–1973.
- [12] Jalaluddin, A. Miyara, Thermal Performances of Vertical Ground Heat Exchangers in Different Conditions, *J. Eng. Sci. Technol.* 11 (2016) 1771–1783.
- [13] Jalaluddin, R. Tarakka, A. Miyara, Performance of Shallow Borehole of spiral-Tube Ground Heat Exchanger, *J. Mech. Eng.* 15 (2018) 41–52.

-
- [14]Jalaluddin, A. Miyara, S. Ishikawa, R. Tarakka, A.A. Mochtar, Development of an open-loop ground source cooling system for space air conditioning system in hot climate like Indonesia, MATEC Web Conf. 204 (2018) 04007.
- [15]Jalaluddin, E. Arif, R. Tarakka, Experimental Study of an SWH System with V-Shaped Plate, J. Eng. Technol Sci. 48 (2016) 11.
- [16]Jalaluddin, R. Tarakka, M. Rusman, A.A. Mochtar, Performance Investigation of Solar Water Heating System with V-Shaped Absorber Plate Integrated PCM Storage. Int. J. Eng. Appl. IREA. 8 (2020).
- [17]C.C. Chen, P.C. Huang, Numerical study of heat transfer enhancement for a novel flat-plate solar water collector using metal-foam blocks. Int. J. Heat Mass Transf. 55 (2012) 6734–6756.



CERTIFICATE OF PRESENTER

The certificate presented to:

Muhammad Hasan Basri

Has participated with a paper entitled

Thermal Properties Characteristic of Aluminium-Alumina for Solar Water Heating System Application

At *The International Symposium on Advance and Innovation in Mechanical Engineering (ISAIME) 2022* held on October 13 , 2022 by Mechanical Engineering Departement of Universitas Hasanuddin in collaboration with Badan Kerja Sama Teknik Mesin Indonesia (BKS-TM Indonesia)

Makassar, October 13 , 2022

